Energy of the bosonic kinks in the quasiparticle spectrum of cuprate superconductors

E. Schachinger[1,*] and J. P. Carbotte[2,3]
[1]*Institute of Theoretical and Computational Physics, Graz University of Technology, A-8010 Graz, Austria*
[2]*Department of Physics and Astronomy, McMaster University, Hamilton, Ontario, Canada N1G 2W1*
[3]*The Canadian Institute for Advanced Research, Toronto, Ontario, Canada M5G 1Z8*
(Received 11 February 2009; revised manuscript received 18 June 2009; published 23 September 2009)

Kinks seen in the renormalized electronic dispersion curves of the cuprates have been widely interpreted as due to coupling to bosonic excitations. The relationship between boson energy and the kink position can depend on temperature, the state of the electronic system, superconducting or normal, as well as on the shape of the underlying electron-boson interaction spectral density. Only in the unrealistic case of a Dirac δ-function spectral density does the kink energy correspond to the sum of the boson energy plus the superconducting gap.

DOI: 10.1103/PhysRevB.80.094521 PACS number(s): 74.20.Mn, 74.72.−h

I. INTRODUCTION

Angular-resolved photoemission spectroscopy (ARPES) has been widely used to measure the renormalized electronic dispersion curves in the high-T_c cuprates. So-called "kinks" are seen in these dispersion curves[1–4] which are believed to be due to coupling to particular boson modes although the exact nature of these excitations remains controversial. Some argue for phonons[1,4] while others favor spin fluctuations.[2,3] This is an important issue in its own right but does not impact directly on the present work. Whatever their origin, it is expected[5] that the resulting kinks should shift in energy due to the opening of a superconducting gap for the nodal-direction dispersion curves. Several nodal-direction measurements,[5–7] however, find little or no such shifts, an observation that has been considered anomalous. In a recent paper Lee *et al.*[5] studied single crystals of optimally doped $Bi_2Sr_2Ca_{0.92}Y_{0.08}Cu_2O_{8+\delta}$ (Bi2212) with a $T_c=96$ K with the direct aim of addressing this puzzle. In their analysis several δ-functions are employed to characterize the electron-boson spectral density and they use the fact that the structures in the nodal-direction dispersion curves caused by these δ-functions are shifted in energy by the superconducting gap below T_c. Moreover, they argue that two phonons are involved which differ in energy exactly by the gap value with the high-energy feature dominant in the normal state and vice versa in the superconducting state. Here we study a different aspect of the problem which provides insight into superconductivity-induced boson shifts. We will find that for extended electron-boson spectral densities which will be denoted by $I^2\chi(\omega)$, a peak in this function does not correspond to a feature in the dispersion curves which shifts in energy by the full gap. Rather the amount of shift involved is sensitive to the shape of $I^2\chi(\omega)$ as well as to the value of the gap, and, in the normal state where the gap $\Delta(T)=0$, it depends on temperature T.

ARPES data shows that the renormalization caused by the spectral density $I^2\chi(\omega)$ can depend significantly on direction,[8] nodal or antinodal, for example. In our formulation this translates into the fact that the spectral density itself depends on the direction of the quasiparticle (QP) momentum $\mathbf{k}$. This dependence on angle arises because electronic-scattering processes depend on initial and not only on final states over which an average is taken. For instance, Fermi surface to Fermi-surface scattering processes involving an excitation of momentum (π,π), whatever its origin, might not be possible in the nodal direction yet become more likely as the antinodal direction is approached. This arises because of the particular geometry of the Fermi surface involved in the cuprates.

Section II presents results for the QP self-energy based on model spectra while Sec. III deals with the renormalized QP energies measured in ARPES experiments. In Sec. IV we present additional results based on realistic spectra obtained from inversions of optical as well as nodal-direction ARPES data. A summary and conclusions are found in Sec. V.

II. SELF-ENERGY BASED ON MODEL SPECTRA

The dressed dispersion relation of the charge carriers depends on the real part of the QP self-energy, $\Sigma_1(\omega)$, which is given by[9–12]

$$\Sigma_1(\omega,T)=P\int_0^\infty d\Omega I^2\chi(\Omega)\int_{-\infty}^{\infty}d\nu\tilde{N}(\nu,T)\times\left[\frac{n(\Omega,T)+f(-\nu,T)}{\omega-\Omega-\nu}+\frac{n(\Omega,T)+f(\nu,T)}{\omega+\Omega-\nu}\right],\tag{1}$$

where P denotes the principal part integral, $\tilde{N}(\nu,T)$ is the self-consistent superconducting state electronic density of states (DOS), $n(\Omega,T)$ and $f(\nu,T)$ are the Bose and Fermi temperature factors, respectively. This expression holds for any system with effective DOS $\tilde{N}(\nu,T)$ and electron-boson spectral density $I^2\chi(\omega)$. The formalism on which this formulation is based is Eliashberg theory first considered for an electron-phonon system[13] but also widely used in the nearly antiferromagnetic Fermi-liquid model based on spin fluctuations as reviewed by Chubukov *et al.*[14] We have assumed, for simplicity, particle-hole symmetry. To begin we consider the limit of zero temperature, $T=0$, and also take the self-consistent electronic DOS to be constant, namely, $\tilde{N}(\nu)=1$. Equation (1) can then be written as a convolution integral and its derivative is given by

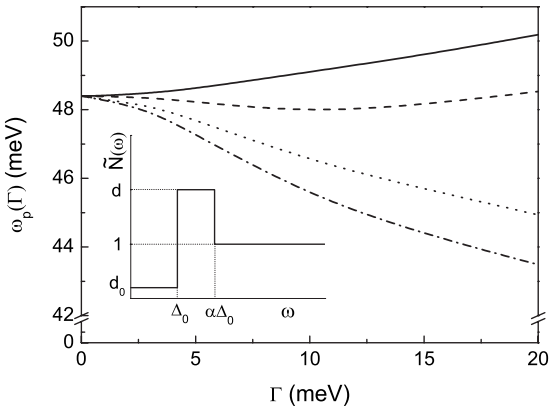

FIG. 1. Position of the peak ω_p in the real part of the QP self-energy $-\Sigma_1(\omega)$ as a function of the width Γ of a Lorentzian model for $I^2\chi(\omega)$ and for $T=0$. The inset gives the model DOS $\tilde{N}(\omega)$ equal to d_0 for $|\omega|<\Delta_0$, to d for $\Delta_0\leq|\omega|\leq\alpha\Delta_0$ (the recovery region), and to one for $|\omega|>\alpha\Delta_0$ (background region). Results are presented for $d_0=0$, $d=1$, $\alpha=0$ (solid line), $d_0=0.2$, $d=1$, $\alpha=0$ (dashed line), $d_0=0$, $d=2$, $\alpha=2$ (dotted line), and $d_0=0.2$, $d=2$, $\alpha=1.8$ (dashed-dotted line).

$$\frac{d\Sigma_1(\omega)}{d\omega}=P\int_0^\infty d\Omega h(\Omega,\omega)I^2\chi(\Omega), \tag{2}$$

with $h(\Omega,\omega)=-2\Omega/(\Omega^2-\omega^2)$. For a given value of ω this function of Ω, diverges at $\Omega=\omega$, is positive for $\Omega<\omega$ and negative for $\Omega>\omega$. To get $d\Sigma_1(\omega)/d\omega=0$ requires the area under the overlap of $h(\Omega,\omega)$ and $I^2\chi(\Omega)$ to vanish. For a δ-function spectrum centered around ω_L this occurs at $\omega=\omega_p=\omega_L$. Adding weight to the spectrum at energies $\Omega>\omega_L$ necessarily implies $\omega_p>\omega_L$ so as to keep the balance between $h(\Omega,\omega)$ and $I^2\chi(\Omega)$. The opposite, $\omega_p<\omega_L$, occurs when weight is added to the spectrum at energies $\Omega<\omega_L$. We can also show that (proof not presented here) for any spectrum symmetric about ω_L, the peak position ω_p will always be greater than ω_L as we will see in the numerical work presented below.

Next we consider the case when there is a gap in the self-consistent DOS. The simplest model is $\tilde{N}(\omega)=0$ for $|\omega|\leq\Delta_0$ and $\tilde{N}(\omega)=1$ otherwise. The origin of the gap Δ_0 is unspecified at this stage. Equation (2) still applies with the kernel shifted to $h(\Omega+\Delta_0,\omega)$. For a δ-function spectral density $I^2\chi(\Omega)=A\delta(\Omega-\omega_L)$, with A its area, we get $d\Sigma_1(\omega)/d\omega=Ah(\omega_L+\Delta_0,\omega)$ which changes from $-\infty$ to $+\infty$ at $\omega_p=\Delta_0+\omega_L$ where it also goes through zero and, thus, the sum of gap plus boson energy determines the peak position in $-\Sigma_1(\omega)$. If, however, $I^2\chi(\Omega)$ is a distributed spectral density represented, for instance, by a cutoff Lorentzian form of width Γ and central frequency ω_L, the peak ω_p in $-\Sigma_1(\omega)$ is no longer at $\Delta_0+\omega_L$ as shown by the solid curve in Fig. 1. The parameters used are $\Delta_0=12$ meV, $\lambda=2\int_0^\infty d\Omega I^2\chi(\Omega)/\Omega=1.2$, $\omega_L=36.4$ meV, and $T=0$. As Γ is increased ω_p increases above its δ-function plus superconducting gap value of 48.4 meV. Even if we assumed $\Delta_0=0$ (the no gap case) $\omega_p>\omega_L$ for any finite value of Γ. In this sense the Dirac δ-function case is anomalous and will never arise in real systems.

Another useful model for the self-consistent DOS, $\tilde{N}(\omega)$ (shown in the inset of Fig. 1), is to take it to be d_0 for $|\omega|\leq\Delta_0$, d for $\Delta_0\leq|\omega|\leq\alpha\Delta_0$ and one beyond this. The first region allows for the possibility that not all states are removed below Δ_0 and the second region is called the state recovery region. To conserve states $(1-d_0)=(d-1)(\alpha-1)$ with $d_0<1$ and $d,\alpha>1$. But we will not always enforce state conservation so that we can assess separately the effect on ω_p of each of the parameters d_0, d, and α. The dashed curve in Fig. 1 for $d_0=0.2$, $d=1$, and $\alpha=0$ shows that when some states remain below the gap, ω_p is reduced from its value when there are none. The dotted curve for $d_0=0$ and $d=\alpha=2$ corresponds to the case of no states below the gap but state conservation applies with the displaced states distributed evenly in the region $\Delta_0\leq|\omega|\leq2\Delta_0$ above the gap. In this case ω_p gets significantly reduced as Γ is increased. The reduction is even greater in the dashed-dotted curve which has states in the gap region ($d_0=0.2$) and the recovery region extends only to $1.8\Delta_0$. It is quite clear from the study of these simple cases that one cannot expect the rule $\omega_p=\omega_L+\Delta(T)$ to hold for realistic DOS and electron-boson spectral densities not described by δ-functions.

Next we present results for the superconducting state described by generalized Eliashberg equations[11,12] to account for d-wave gap symmetry. For simplicity the same Lorentzian spectral density is used in both renormalization and gap channels. Since we keep $\omega_L=36.4$ meV and $\lambda=1.2$ the critical temperature and the superconducting gap amplitude will change with the width Γ of the Lorentzian spectrum, as indicated in Fig. 2(a). The solid squares give the position of the peak $\omega_p(\Gamma)$ in minus the real part of the QP self-energy which is shown in Fig. 2(b), for several values of Γ at $T=3$ K. These solid squares are to be compared with the solid circles for the sum $\omega_L+\Delta$ which in all cases fall above the values of ω_p. For $\Gamma=20$ meV, for instance, ω_p is shifted above ω_L by only 46% of the gap Δ. It is clear that for extended spectra the shift is never equal to the full gap and can be much less.

Note that the solid line in Fig. 2(b) for $\Gamma=1$ meV shows a nearly vertical drop at an energy which corresponds exactly to $\omega_L+\Delta$ and that ω_p falls slightly below this energy. For the special case of a δ-function spectral density $I^2\chi(\Omega)$, however, ω_p would be exactly equal to $\omega_L+\Delta$. This feature can easily be understood from the mathematical structure of Eq. (1). Taking $T=0$ and $I^2\chi(\Omega)=A\delta(\Omega-\omega_L)$ we see that Eq. (1) contains a singular term of the form $AP\int_{-\infty}^{\infty}d\nu\frac{\tilde{N}(\nu)}{\omega-\omega_L-\nu}$, which is, however, integrable. For a superconductor $\tilde{N}(\nu)$ will have a large peak (logarithmic singularity for d wave and inverse square-root singularity for s-wave gap symmetry) at $\nu=\Delta(T)$ which ensures that the maximum in this integral is exactly at $\omega=\omega_L+\Delta(T)$. This rule, however, is special to the δ-function case as we see in Fig. 2(b).

After having studied the influence of the Lorentzian width Γ on the peak position at $T=0$ and 3 K we will now concentrate on the influence the temperature has on ω_p. To accomplish this task we concentrate on a Lorentzian model spectral density with $\Gamma=3$ meV, $\lambda=1.2$, and $\omega_L=36.4$ meV. Solu-

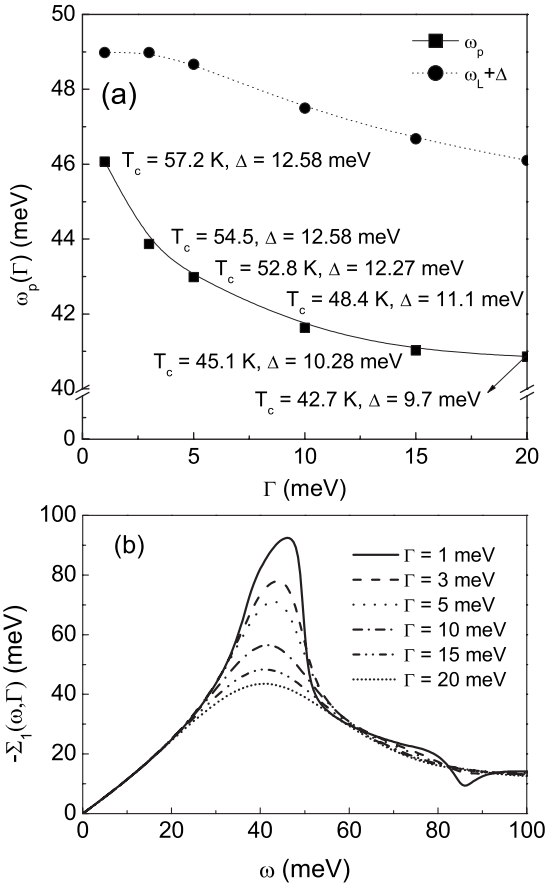

FIG. 2. (a) Position of peak $\omega_p(\Gamma)$ (solid squares) in minus the real part of the QP self-energy as a function of the width Γ of the Lorentzian model for $I^2\chi(\omega)$ with ω_L=36.4 meV, λ is fixed at 1.2, and T=3 K. The solid circles are the boson energy ω_L plus the gap amplitude Δ. The critical temperature and gap vary as indicated. (b) Minus the real part of the QP self-energy $-\Sigma_1(\omega)$ vs energy ω for various values of Γ.

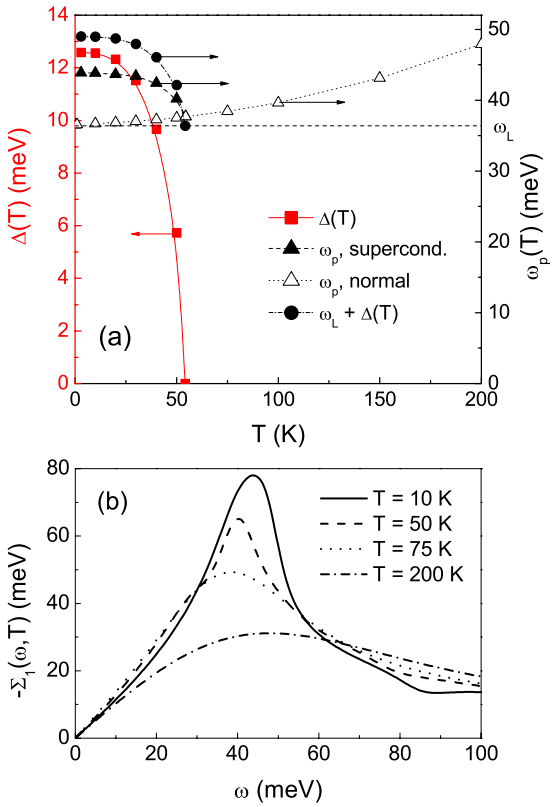

FIG. 3. (Color online) (a) Position $\omega_p(T)$ of the peak in minus the real part of the QP self-energy as a function of temperature T for a Lorentzian model $I^2\chi(\omega)$ with central frequency ω_L=36.4 meV, width Γ=3 meV and λ=1.2, giving T_c=54.5 K. The solid triangles are in the superconducting state and the open triangles are the normal state. (Right-hand scale.) The lines are guides to the eye. The (red) solid squares (left-hand scale) are the gap $\Delta(T)$ vs T and the solid (black) circles are $\omega_p=\omega_L+\Delta(T)$. (b) Minus the real part of the QP self-energy, $-\Sigma_1(\omega)$ vs energy ω for four temperatures, namely, T=10 K (solid line), T=50 K (dashed line), T=75 K (dotted line), and T=200 K (dashed-dotted line).

tions of the Eliashberg equations generalized to include d-wave gap symmetry give in this case a T_c=54.5 K and the superconducting gap amplitude $\Delta(T)$ obtained as a function of temperature below T_c is shown as (red) solid squares in Fig. 3(a) to which the left-hand scale applies. From the Eliashberg solutions we have also evaluated the QP self-energy at temperature T. The real part of $-\Sigma(\omega)$ is shown in Fig. 3(b) for four temperatures. The corresponding maxima in $-\Sigma_1(\omega)$ are plotted as the (black) solid triangles [Fig. 3(a)] for the superconducting state and as the open triangles for the normal state. For ease of comparison we also plotted, using solid (black) circles, the quantity $\omega_L+\Delta(T)$ which in all cases falls above the value of $\omega_p(T)$ in the superconducting state. The shift in $\omega_p(T)$ upon condensation is never the full $\Delta(T)$ but rather 60–65 % of $\Delta(T)$ in the particular case considered. In the normal state ω_p increases considerably with increasing temperature although ω_L is held fixed and there is no gap. Note how the increase in ω_p with temperature partially compensates the effect of the reduction in $\Delta(T)$ on its value. Thus, $\omega_p(T)$ varies less than does $\omega_L+\Delta(T)$.

III. RENORMALIZED QUASIPARTICLE ENERGIES

One could wonder if the position of the peak in the dressed dispersion curves is exactly the same as the corresponding peak in the QP self energy. This is addressed in Fig. 4 which has two frames. In Fig. 4(a) we show the dressed dispersion denoted by $\varepsilon(\omega)$ as a function of the bare energy ω (light, short dotted line) for several temperatures in the normal and superconducting state as labeled in the figure. In Fig. 4(b) we compare the position of the peak in $\varepsilon(\omega)$ denoted by ε_p with the position of the peak in $-\Sigma_1(\omega)$ denoted by ω_p as a function of temperature for our Lorentzian model with ω_L=36.4 meV, Γ=3 meV, and λ=1.2. While they track each other they are not quite the same. As we found for the peak position in the QP self-energy, ε_p can also be quite a bit smaller than $\omega_L+\Delta(T)$ which is indicated by solid circles in Fig. 4(b).

Returning to the solid (red) curve in Fig. 4(a) a second energy scale can be identified (in addition to the energy associated with the peak in the QP dispersion curve), namely, the midpoint of the sharp drop (edge) in this curve which

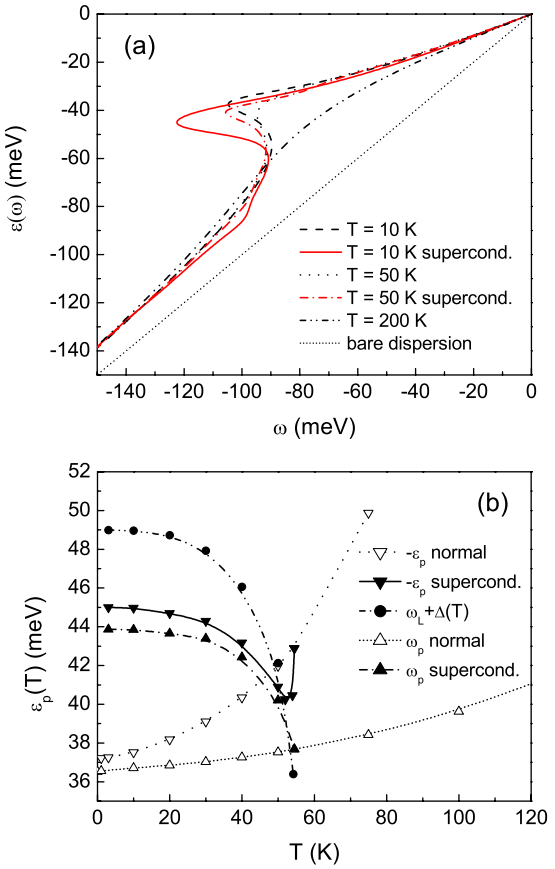

FIG. 4. (Color online) (a) The renormalized electron dispersion relation $\varepsilon(\omega)$ as a function of bare energy ω which plays the role of momentum in our calculations. We present results for three temperatures, namely, $T=10$ K [(red) solid line for the superconducting state and (black) dashed line for the normal state], $T=50$ K [(red) dashed-dotted line for the superconducting state and (black) dotted line for the normal state], and $T=200$ K. (b) Comparison of the peak position in the renormalized dispersion curve, ε_p with the peak position ω_p in the real part of the QP self-energy as a function of temperature T. The solid down triangles indicate the superconducting state results for ε_p while the open down triangles are for the normal state. The solid and open up triangles indicate the results for ω_p and are identical to the results discussed in Fig. 3(a). Finally, the solid circles correspond to $\omega_L+\Delta(T)$.

identifies the rapid decrease toward its unrenormalized value [$\Sigma_1(T,\omega)$ rapidly becomes smaller].[15] We have verified that this energy which falls below the peak energy ϵ_p also varies much less than the superconducting gap for $0<T<T_c$. Only in the artificial case of a δ-function spectral density $I^2\chi(\omega)$ do all these energies coincide.

IV. REALISTIC SPECTRA

So far we have used Lorentzian forms for the electron-boson spectral function $I^2\chi(\omega)$. Realistic forms for this function are now known from maximum entropy inversions of nodal-direction ARPES data[7,11,16,17] as well as from optical data.[18–21] The data of Zhang *et al.*[7] were obtained with a laser-based ARPES technique claiming to have superhigh

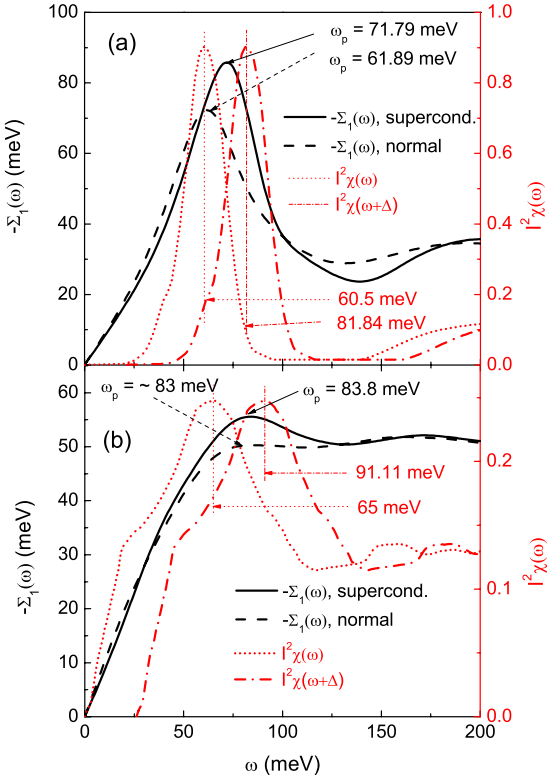

FIG. 5. (Color online) (a) Minus the real part of the QP self-energy, $-\Sigma_1(\omega)$ vs energy ω. Black solid (superconducting state) and dashed lines (normal state) are for $T=27$ K (left-hand scale). Also, shown are $I^2\chi(\omega)$ (dotted line) and $I^2\chi(\omega+\Delta)$ (dashed-dotted line) based on the optical data of Ref. 19 (right-hand scale). (b) Same as (a) for $T=17$ K and based on the $I^2\chi(\omega)$ obtained from nodal-direction Bi2212 ARPES data (Ref. 11).

resolution. The material is optimally doped Bi2212 in which they resolve new high-energy features at ~115 and ~150 meV as well as the known feature at ~70 meV. Inversion of this data to recover the electron-boson spectral density $I^2\chi(\omega)$ gives the (red) dotted curve of Fig. 5(b) with a prominent peak at ~65 meV. Its width is rather broad and is certainly far from a δ-function or from a Lorentzian form as are the spectra derived from optics shown as the (red) dotted line in Fig. 5(a).

In this figure we show results for the real part of the nodal-direction QP self-energy $-\Sigma_1(\omega)$ as a function of ω. Left-hand vertical scale applies. The (black) solid curve is in the superconducting state and the (black) dashed curve is in the normal state. The model spectral density on which these results are based is shown as the (red) dotted line and its displaced value $I^2\chi(\omega+\Delta)$ as the (red) dashed-dotted line. The right-hand scale applies. The $I^2\chi(\omega)$ has been derived from optics[19] and was scaled down by a factor of 0.5 following the argument given in Ref. 11. Figure 5(a) is for $T=27$ K. The gap at this temperature $\Delta=21.34$ meV in our numerical solutions of the finite band Eliashberg equations (bandwidth 1.2 eV) while the shift in peak position of $-\Sigma_1(\omega)$ between superconducting and normal state is only ~10 meV which is less than half the gap value. Note that in this case the peak in $I^2\chi(\omega)$ at ~60 meV is much more prominent and well separated from the high-energy back-

ground as compared with the ARPES derived spectra[11] used in Fig. 5(b) [(red) dashed and dashed-dotted lines, right-hand scale]. While this second spectrum has a peak around 65 meV its height above the background is of the same order as the background itself which extends to high energies (~400 meV) which is the energy at which the dressed and undressed dispersion relations are assumed to cross. Consequently, the maximum in $-\Sigma_1(\omega)$ corresponds to such a very weak structure that it would be very hard to determine its position in energy accurately, particularly in the normal state (dashed line). Here we find no significant peak shift between solid and dashed curves.

In a recent experiment Iwasawa *et al.*[22] found a shift in the peak around 70 meV in an oxygen isotope substituted sample of Bi2212 indicating that phonons are responsible for this structure. While, as we have stated before, the present work deals mainly with the correspondence between a structure in $I^2\chi(\omega)$ and its signature in the electronic dispersion curves, the question of the origin of the boson structure is certainly important. Through detailed calculations we have established[23] that the data of Ref. 22 can be understood if we assume that the peak above background of Fig. 5(b) [(red) dotted curve] is entirely due to phonons with the reminder from some other source. This peak involves ~10% of the total area under $I^2\chi(\omega)$. We note that the authors identify the phonon by an Einstein mode and its energy, ω_E is determined from the peak in the real part of the QP self-energy using either $\omega_p=\omega_E+\Delta$ or simply $\omega_p=\omega_E$.

V. SUMMARY

At zero temperature, for a δ-function electron-boson spectral density centered at ω_L, the real part of the QP self-energy $-\Sigma_1(\omega)$ will have a maximum precisely at $\omega_p=\omega_L$ in the normal state and at $\omega_p=\omega_L+\Delta_0$ in the superconducting state with gap Δ_0. For a distributed electron-boson spectrum this rule no longer holds. Even for the normal state with a flat electronic DOS, ω_p will increase with increasing temperature and for the superconducting state $\omega_p(T)$ will be less than $\omega_L+\Delta(T)$. Based on a narrow Lorentzian model for $I^2\chi(\omega)$ we find the superconductivity-induced shifts are of the order of half rather than the full gap with their exact value depending on the details of the particular case. For realistic spectra derived from maximum entropy inversions of nodal-direction ARPES data or, alternatively, from optical data it is found that the shift can be even less than 1/3 of the gap. If the maximum in $I^2\chi(\omega)$ is rather broad as in the ARPES derived data the superconductivity-induced shift of ω_p is practically negligible. While phonons are not expected to change much with temperature and between normal and superconducting state other bosons could.

ACKNOWLEDGMENTS

Research supported in part by the Natural Sciences and Engineering Research Council of Canada (NSERC) and by the Canadian Institute for Advanced Research (CIFAR). We thank T. Timusk for interest.

*schachinger@itp.tu-graz.ac.at

[1] P. V. Bogdanov, A. Lanzara, S. A. Kellar, X. J. Zhou, E. D. Lu, W. J. Zheng, G. Gu, J. I. Shimoyama, K. Kishio, H. Ikeda, R. Yoshizaki, Z. Hussain, and Z. X. Shen, Phys. Rev. Lett. **85**, 2581 (2000).

[2] A. Kaminski, M. Randeria, J. C. Campuzano, M. R. Norman, H. Fretwell, J. Mesot, T. Sato, T. Takahashi, and K. Kadowaki, Phys. Rev. Lett. **86**, 1070 (2001).

[3] P. D. Johnson, T. Valla, A. V. Fedorov, Z. Yusof, B. O. Wells, Q. Li, A. R. Moodenbaugh, G. D. Gu, N. Koshizuka, C. Kendziora, Sha Jian, and D. G. Hinks Phys. Rev. Lett. **87**, 177007 (2001).

[4] A. Lanzara, P. V. Bogdanov, X. J. Zhou, S. A. Kellar, D. L. Feng, E. D. Lu, T. Yoshida, H. Eisaki, A. Fujimori, K. Kishio, J.-I. Shimoyama, T. Noda, S. Uchida, Z. Hussain, and Z.-X. Shen, Nature (London) **412**, 510 (2001).

[5] W. S. Lee, W. Meevasana, S. Johnston, D. H. Lu, I. M. Vishik, R. G. Moore, H. Eisaki, N. Kaneko, T. P. Devereaux, and Z. X. Shen, Phys. Rev. B **77**, 140504(R) (2008).

[6] T. Sato, H. Matsui, T. Takahashi, H. Ding, H. B. Yang, S. C. Wang, T. Fujii, T. Watanabe, A. Matsuda, T. Terashima, and K. Kadowaki, Phys. Rev. Lett. **91**, 157003 (2003).

[7] W. Zhang, G. Liu, L. Zhao, H. Liu, J. Meng, X. Dong, W. Lu, J. S. Wen, Z. J. Xu, G. D. Gu, T. Sasagawa, Guiling Wang, Yong Zhu, Hongbo Zhang, Yong Zhou, Xiaoyang Wang, Zhongxian Zhao, Chuangtian Chen, Zuyan Xu, and X. J. Zhou, Phys. Rev. Lett. **100**, 107002 (2008).

[8] T. Cuk, F. Baumberger, D. H. Lu, N. Ingle, X. J. Zhou, H. Eisaki, N. Kaneko, Z. Hussain, T. P. Deveraux, N. Nagaosa, and Z.-X. Shen, Phys. Rev. Lett. **93**, 117003 (2004).

[9] B. Mitrović and J. P. Carbotte, Can. J. Phys. **61**, 758 (1983).

[10] A. Knigavko and J. P. Carbotte, Phys. Rev. B **72**, 035125 (2005).

[11] E. Schachinger and J. P. Carbotte, Phys. Rev. B **77**, 094524 (2008).

[12] J. P. Carbotte, E. Schachinger, and J. Hwang, Phys. Rev. B **71**, 054506 (2005).

[13] J. P. Carbotte, Rev. Mod. Phys. **62**, 1027 (1990).

[14] A. V. Chubukov, D. Pines, and J. Schmalian, in *Superconductivity, Conventional and Unconventional Superconductors*, edited by K. H. Bennemann and J. B. Ketterson (Springer, New York, 2004), Vol. 2, p. 1349.

[15] A. W. Sandvik, D. J. Scalapino, and N. E. Bickers, Phys. Rev. B **69**, 094523 (2004).

[16] J. Shi, S. J. Tang, B. Wu, P. T. Sprunger, W. I. Yang, V. Bruet, Z. X. Zhou, Z. Hussain, Z. X. Shen, Z. Zhang, and E. W. Plummer, Phys. Rev. Lett. **92**, 186401 (2004).

[17] X. J. Zhou, J. Shi, T. Yoshida, T. Cuk, W. L. Yang, V. Bruet, J. Nakamura, N. Manella, S. Komiya, Y. Ando, F. Zhou, W. X. Ti, J. W. Xiong, Z. X. Zhao, T. Sasagawa, T. Kakeshita, H. Eisaki, S. Uchida, A. Fujimori, Zhenyu Zhang, E. W. Plummer, R. B. Laughlin, Z. Hussain, and Z.-X. Shen, Phys. Rev. Lett. **95**, 117001 (2005).

[18] E. Schachinger, D. Neuber, and J. P. Carbotte, Phys. Rev. B **73**, 184507 (2006).

[19] J. Hwang, T. Timusk, E. Schachinger, and J. P. Carbotte, Phys. Rev. B **75**, 144508 (2007).
[20] J. Hwang, E. Schachinger, J. P. Carbotte, F. Gao, D. B. Tanner, and T. Timusk, Phys. Rev. Lett. **100**, 137005 (2008).
[21] E. Schachinger, C. C. Homes, R. P. S. M. Lobo, and J. P. Carbotte, Phys. Rev. B **78**, 134522 (2008).
[22] H. Iwasawa, J. Douglas, K. Sato, T. Masui, Y. Yoshida, Z. Sun, H. Eisaki, H. Bando, A. Ino, M. Arita, K. Shimada, H. Namatame, M. Taniguchi, S. Tajima, S. Uchida, T. Saitoh, D. S. Dessau, and Y. Aiura, Phys. Rev. Lett. **101**, 157005 (2008).
[23] E. Schachinger, J. P. Carbotte, and T. Timusk, EPL **86**, 67003 (2009).